Photoelectron Spectroscopy of Alkali Metal Cluster Anions

J.G. Eaton, L.H. Kidder, H.W. Sarkas, K.M. McHugh, and K.H. Bowen[1]

[1]Department of Chemistry
The Johns Hopkins University
Baltimore, MD 21218 USA

ABSTRACT

We present the photoelectron (photodetacment) spectra of K^-_{2-19} recorded using 2.540 eV photons. These spectra are highly structured, providing a wealth of information about the electronic structure of alkali metal clusters, including adiabatic electron affinities and electronic splittings for each size. Spectral assignments have been made with guidance from theory. For the smaller cluster sizes, detailed assignments of the spectra were aided by *ab initio* quantum chemical calculations. For the larger clusters, assignments were guided by a simple shell model. A substantial correlation is found between the predicted shell model energy levels and the observed patterns and spacings in the spectra.

1. Introduction

Among metal cluster anions, alkali metal cluster anions offer relative simplicity, and their photoelectron spectra exhibit unusual clarity. Alkali atoms are hydrogen-like, each with a s^1 valence electron and a rare gas electron core configuration. Bulk alkali metals are the simplest of metals, being essentially free electron metals. Because of these simplifying characteristics at the extrema of size, alkali metal clusters in the vast size regime between a single atom and the condensed phase offer unique opportunities for better understanding the electronic properties of metal aggregates generally.

Interest in alkali metal clusters has generated a rich literature pertaining not only to theoretical[1-11] and experimental[12-20] studies of neutral and cationic alkali clusters, but also to a lesser extent to theoretical[21-25] and experimental[26,27] work on alkali cluster anions. Negative ion photoelectron studies of metal cluster anions comprised of s^1 atoms have included work on metal cluster anions of the coinage metals by Lineberger[28,29], Meiwes-Broer[30], and Smalley[31] and on small alkali cluster anions by our group[27]. Here, we extend our previous work on alkali cluster anions and present the phototelectron (photodetachment) spectra of potassium cluster anions, K^-_n, with n = 2 -19.

2. Experimental

Negative ion photoelectron spectroscopy is conducted by crossing a mass-selected beam of negative ions with a fixed-frequency photon beam and energy analyzing the resultant photodetached electrons. The main elements of our negative ion photoelectron spectrometer are (a) an ion beam line along which negative ions are formed, transported, and mass-selected by an

E × **B** Wien filter, (b) an argon ion laser which is operated intracavity in the ion/photon interaction region, and (c) a magnetically shielded, high resolution hemispherical electron energy analyzer, located below the plane of the crossed ion and photon beams. A particularly important attribute of this technique is its ability to size-select cluster anions before photodetachment so that photoelectron spectra of individual cluster anion sizes can be recorded.

To generate beams of potassium cluster anions, we use a heated supersonic expansion ion source. In this device, the stagnation chamber is divided into separately heated oven reservoir and nozzle channel sections. The alkali metal is heated in the oven to a temperature corresponding to several hundred torr equilibrium vapor pressure. The vapor is then coexpanded with several hundred torr of argon into high vacuum through the nozzle, which is maintained ~50 degrees hotter than the oven. Finally, a negatively biased hot filament injects low energy electrons directly into the expanding jet in the presence of axial magnetic fields, producing potassium cluster anions.

3. Results

The photoelectron spectra of K^- and the potassium cluster anions, $K^-_{2\text{-}19}$ are presented in Figure 1. These spectra were recorded with 2.540 eV photons. The photoelectron spectra of alkali cluster anions are highly structured, an attribute that derives both from the inherent properties of the alkalis and from the available electron energy resolution (~30 meV) of our spectrometer. The individual peaks in these spectra arise due to photodetachment transitions between the ground electronic state of a given cluster anion and the ground and various energetically-accessible excited electronic states of its corresponding neutral cluster. Thus, one learns two main kinds of information from an analysis of these spectra, ie., adiabatic electron affinity values and electronic structure data, both as a function of cluster size. Adiabatic electron affinities for metal clusters are expected to increase with cluster size, reaching the work function of the bulk metal at infinite cluster size. There are two ways of looking at the electronic structure information in these spectra. In the picture alluded to above, the spacings between peaks in a given spectrum reflect the energy splittings between the various electronic states of the neutral cluster, albeit at the geometry of its corresponding cluster anion. In the other view, which is equivalent to the first picture at the Koopmans' theorem level of approximation, the peaks in a given spectrum are ascribed to electrons being removed or plucked from the occupied energy levels of the cluster anion. In this picture, the peak spacings and patterns directly reflect the upper portion of the occupied energy level structure of the cluster anion. In either picture, however, the observed peak structure in these spectra is a manifestation of how the electronic structure of the alkali metal cluster system is evolving as a function of cluster size. Eventually at some larger cluster size, this electronic structure is expected to organize itself into the essentially structureless valence band of bulk potassium metal.

4. Electron Affinities vs. Cluster Size

Adiabatic electron affinities (EA's) were extracted from the spectra and are presented as a function of cluster size in Figure 2. These results exhibit largely an odd-even alternation of electron affinities with cluster size. Using *ab initio* quantum chemistry methods, Bonačić-Koutecký [4] has calculated the adiabatic electron affinities for potassium clusters from sizes n = 2-6. The quantitative agreement of her calculations with our experimental results is rather good. For theoretical guidance at larger potassium cluster sizes, we turned to a qualitative comparison with the predictions of simple shell models. Figure 3 compares our experimentally-determined EA vs. n trend with the qualitative EA vs. n trend predicted by an ellipsoidal shell model. The latter plots the scaled energy of the highest occupied energy level of the cluster

containing n + 1 electrons as a function of cluster size, n. Since a large energy for the highest occupied energy level in the anion implies a relatively low electron affinity, we have inverted the energy scale on our experimental EA vs. n plot to facilitate comparison of these two graphs. It is evident that this shell model reproduces much of the EA vs. n trend found experimentally. Note that an ellipsoidal shell model predicts "peaks" in the EA vs. n trend in Fig. 3 at n = 8, 10, 14, and 18, and that we observe these experimentally. Additionally, however, we also see "peaks" at n = 4 and 12 which are not predicted by this shell model. (Note, of course, that "peaks" in the upper panel of Fig. 3 appear as "dips" in Fig. 2.)

5. Electronic Structure and Spectral Assignments

The photoelectron spectra of alkali metal cluster anions are laden with information about electronic structure, yet their interpretation is not obvious by inspection. Thus, our primary goal at this stage has been to assign these spectra in some rudimentary but useful way. In order to do this we need theoretical support. At relatively small alkali cluster anion sizes, the *ab initio* calculations of Bonačić-Koutecký et al. have been an invaluable guide. Two years ago Bonačić-Koutecký [21] modelled our photoelectron spectra of sodium cluster anions over the size range n = 2-5, and very recently she and her group performed similar calculations on potassium cluster anions ranging in size from n = 2-6. This was done by calculating the photodetachment transitions between several possible (energetically close) geometries of a given cluster anion and the ground and energetically-accessible excited electronic states of its corresponding neutral cluster, with the latter being taken in each case at the geometry of the particular isomer of the cluster anion in question. That is, high level quantum mechanical calculations were separately performed on both the cluster anion and its corresponding neutral cluster, followed by the computation of vertical photodetachmment transitions between them. By comparing the photoelectron spectra predicted in this way with a given experimentally observed alkali cluster anion photoelectron spectrum, a wealth of valuable information was obtained about the geometry (or isomeric geometries) of the alkali cluster anion and about the states involved in each of the observed photodetachment transitions. The success of this approach effectively led to an assignment of the spectra in that it identified the transitions which were involved in each observed spectral peak.

As larger cluster sizes are considered beyond the present range of *ab initio* quantum chemistry treatments, however, one must rely on some other form of theoretical guidance. In our earlier work with alkali cluster anions, we had noticed some intriguing correlations between the peak patterns and spacings of our spectra and the predictions of simple shell models. Consider K_7^- for example, an eight valence electron system. Imagine putting two of these electrons into a "s-like" shell and then the remaining six into a "p-like" shell. Further imagine that in such a small system structural effects (or perhaps crystal field effects) lift the degeneracies of the three p sub-levels, leaving two electrons in each of three closely spaced p levels. Next, imagine removing each of these eight electrons from the cluster anion to their common ionization continuum limit, the energy required to do this in each case being its electron binding energy. That predicts a photoelectron spectrum with three closely spaced peaks at low electron binding energy, followed by a gap, followed by another peak at higher electron binding energy. This is what is observed, and furthermore the 1s-1p splitting is quantitatively close to the prediction of the Clemenger-Nilsson[6,8] model for K_8.

With these correlations to encourage us, we set out to see if a simple shell model could work well enough to aid in the assignment of our spectra. To calculate energy levels from which a predicted shell model "stick spectrum" could be generated, we used a program written by Saunders and Knight[20,32]. Essentially, this calculation treats a three dimensional harmonic oscillator having a single perturbation parameter. In addition to its relative simplicity, it has the advantage of easily being able to accommodate triaxial distortions. Only two parameters had to be fixed, one to set the energy scale and one to set the magnitude of the perturbation. These same two parameter values were then used for calculations on all cluster anion sizes. In this

model the value of one quanta of energy is equal to the 1s-1p splitting in the closed shell system with eight valence electrons, and we set it in accordance with the value of the tentatively assigned 1s-1p splitting in our spectrum of K_7^-. Also in this model, the value of the perturbation parameter is equal to the 1d-2s splitting in the closed shell system with twenty valence electrons, and we chose it in accordance with the tentatively assigned 1d-2s splitting in the spectrum of K_{19}^-. Basically, this is a triaxial shell model parameterized for potassium cluster anions.

This approach allowed us to generate predictive "stick spectra", with distinctive spectral patterns and quantitative splittings, for first approximation comparisons with the observed photoelectron spectra. Figures 4-7 present these calculated "stick-spectra" (along with their level designations and electron occupations) as insets on the photoelectron spectra of K_n^- over the cluster size range, n = 4-19. The correlation between the shell model's "stick spectrum" and the actual spectrum for n = 4 is rather good. For n = 5, however, the correlation is not as good. The predicted 1p peak actually appears as two peaks in the real spectrum. Conceivably, the two degenerate 1p sub-levels could be split by some interaction not in the model to yield the two observed peaks. If so, the predicted value of the 1s-1p splitting would agree fairly well with that in the photoelectron spectrum. For n = 6, the correlation is somewhat more convincing. Two peaks deriving from 1p levels are predicted, but the lifting of the degeneracy of two of the 1p sub-levels would result in three 1p peaks. This is consistent with the observed spectrum. The case of n = 7 has been previewed above. The observed triplet of peaks is suggestive of the 1p level's three-fold degeneracy having been lifted. The case of n = 8 is rather convincing. The above kinds of arguments about 1p sub-levels and peaks are applicable here, but in addition the peak for a 1d level appears on cue at the predicted energy due to the opening of a new shell. Inspection of the n = 9 case is also fairly convincing if one allows the doubly degenerate 1p level to split into a doublet of peaks in the spectrum. The n = 10 case is consistent with the model but by itself is not convincing. The n = 11 case has the predicted number of peaks in the combined 1p and 1d manifolds. In most cases, the suspected 1s-1p splittings observed in the spectra are in reasonable accord with those predicted by the model. On the other hand, the model often does poorly in predicting the lifting of 1p sub-level degeneracies.

At n = 12, we lose sight of the 1s peak, ie., it shifts out beyond our photon range. Also here, 1p and 1d manifolds start to segregate into separate groupings of peaks, the beginning of an important trend. Within the 1p grouping of peaks there are three discernible peaks as predicted by the model. The same situation holds for the 1d grouping of peaks. By n = 13, the valley between the 1p and 1d groupings has become deeper and the two groupings more obvious, even though the spectral sub-structure on each grouping is more difficult to interpret. At n = 14, the spectral sub-structure on each of the two peak groupings is practically gone, but the 1p peak grouping has become clearly distinct from the 1d grouping, resulting in a spectrum having two broadened peaks. At n = 15, the pace of 1p and 1d segregation quickens. This is apparent in the predictions of the model and in the observed spectrum, and the valley between the two peak groupings deepens. The n = 16 case continues the trend as does the n = 17 case. The model predicts n = 17 (an 18 valence electron system) to be a spherical closed shell. By n = 18, the model predicts the appearance of a singly occupied 2s level. It faintly presents itself as a shoulder on the low electron binding energy side of the 1d shell peak grouping. At n = 19 (a 20 valence electron system), the model again predicts a spherical closed shell system. Now, however, the doubly occupied 2s level pops out dramatically as a new peak in the spectrum. The size range between n = 14 and 19 provides the most convincing set of correlations between the spectra and the shell model. We observe that, all else being equal, the correlation between the shell model and the observed spectra tends to be better (1) near shell closings, ie., near the 8, 18, and 20 valence electron systems, and (2) for larger cluster anions than for smaller ones. Indeed, both trends are what one would expect from a shell model for metal clusters. Viewing the evidence as a whole, we are led to the conclusion that there is something to a first approximation assignment of these photoelectron spectra in terms of a simple shell model. This is the first time that shell models have been successfully put to the test at the level of single particle energy levels. Always before, shell models were tested via consequential properties such as EA vs n trends, IP vs n trends, and mass spectral abundance patterns.

Shell models have been the subject of intense interest in cluster physics in recent years, the most famous shell model being the celebrated jellium model. Shell models generally arise as a result of fermions moving in attractive smooth potentials. Thus, even though the Saunders/Knight shell model that we have used here is not a jellium shell model, it is reasonable to expect that it should reproduce some of the gross features of a jellium calculation. To date, however, the predictions of a true jellium calculation have not been compared to the photoelectron spectra of potassium cluster anions. It would be interesting to do so, and we look forward to the availability of theoretical results that will make this possible.

Acknowledgements

It is a pleasure to acknowledge valuable conversations concerning this work with V. Bonačić-Koutecký , W. Knight, W. Saunders, D. Lindsay, J. Koutecky, W. Ekardt, M. Kappes, W. deHeer, E. Poliakoff, J. Pacheco, C. Yannouleas, B. Judd, L. Madansky, and K.-H. Meiwes-Broer. This work was supported by the (U.S.) National Science Foundation under grant number CHE-9007445.

References

1. Konowalow, D.D., and Rosenkrantz, M.E., in J.L. Gole and W.C. Stwalley (eds.), Metal Bonding and Interactions in High Temperature Systems, American Chemical Society, Washington D.C. 3-17 (1982)

2. Cocchini, F., Upton, T.H., and Andreoni, W., J. Chem. Phys. 88 6068-6077 (1988)

3. Martins, J.L., Car, R., and Buttet, J., J. Chem. Phys. 78 5646-5655 (1983)

4. Bonačić-Koutecký V., Fantucci, P., and Koutecký, J., Chem. Rev. 91 1035-1108 (1991)

5. Rao, B.K., Khanna, S.N., and Jena, P., Phys. Rev. B 36 953-960 (1987)

6. Clemenger, K., Phys. Rev. B 32 1359-1362 (1985)

7. Cohen, M.L., Chou, M.Y., Knight, W.D., and de Heer, W.A., J. Phys. Chem. 91 3141-3149 (1987)

8. de Heer, W.A., Knight, W.D., Chou, M.Y., and Cohen, M.L., Solid State Physics 40 93-181 (1987)

9. Röthlisberger, U., and Andreoni, W., J. Chem. Phys. 94 8129-8151 (1991)

10. Ekardt, W., Phys. Rev. B 29, 1558-1564 (1984)

11. Ekardt, W., and Penzar, Z., Phys. Rev. B 38 4273-4276 (1988)

12. Ross, A.J., Crozet, P., Effantin, C., d'Incan, J., J. Phys. B: At. Mol. Phys. 20 6225-6231 (1987)

13. Heinze, J., Schöhle, U., Engelke, F., and Caldwell, C.D., J. Chem. Phys. 87 45-53 (1987)

14. Gole, J.L., in M. Moskovits (ed.), Metal Clusters, Wiley, New York 131-184 (1986)

15. Kappes, M.M., Kunz, R.W., and Schumacher, E., Chem. Phys. Lett. 91 413-418 (1982)

16. Pollack, S., Wang, C.R.C., and Kappes, M.M., J. Chem. Phys. 94 2496-2501 (1991)

17. Brechignac, C., Cahuzac, Ph., and Roux, J. Ph., J. Chem. Phys. 87 229-238 (1987)

18. Lindsay, D.M., Herschbach, D.R., and Kwiram, A.L., Mol. Phys. 32 1199-1213 (1976)

19. Delacretaz, G., Grant, E.R., Whetten, R.L., Woste, L., and Zwanziger, J.W., Phys. Rev. Lett. 56 2598-2601 (1986)

20. Selby, K., Kresin, V., Masui, J., Vollmer, M., de Heer, W.A., Scheidemann, A., and Knight, W.D., Phys. Rev. B 43 4565-4572 (1991)

21. Bonačić-Koutecký V., Fantucci, P., and Koutecký, J., J. Chem. Phys. 91 3794-3795 (1989)

22. Rao, B.K., and Jena, P., Int. Jour. of Quant. Chem.: Quant. Chem. Symp. 22 287-296 (1988)

23. Lindsay, D.M., Chu, L., Wang, Y., George, T.F., J. Chem. Phys. 87 1685-1689 (1987)

24. Ortiz, J.V., J. Chem. Phys. 89 6353-6356 (1988)

25. Gole, J.L., Childs, R.H., Dixon, D.A., and Eades, R.A., J. Chem. Phys. 72 6368-6375 (1980)

26. Lelyter, M., and Joyes, P., J. Phys (Paris) 35 L85-L88 (1974)

27. McHugh, K.M., Eaton, J.G., Lee, G.H., Sarkas, H.W., Kidder, L.H., Snodgrass, J.T., Manaa, M.R., and Bowen, K.H., J. Chem. Phys. 91 3792-3793 (1989)

28. Ho, J., Ervin, K.M., and Lineberger, W.C., J. Chem. Phys. 93 6987-7002 (1990)

29. Leopold, D.G., Ho, J., and Lineberger, W.C., J. Chem. Phys. 86 1715-1726 (1987)

30. Ganteför, G., Gausa, M., Meiwes-Broer, K.H., and Lutz, H., Farad. Disc. Chem. Soc. 86 1-12 (1988)

31. Pettiette, C.L., Yang, S.H., Craycraft, M.J., Conceicao, J., Laaksonen, R.T., Chesnovsky, O., and Smalley, R.E., J. Chem. Phys. 88 5377-5382 (1988)

32. Saunders, W.A., Ph. D. Thesis, University of California, Berkeley (1986)

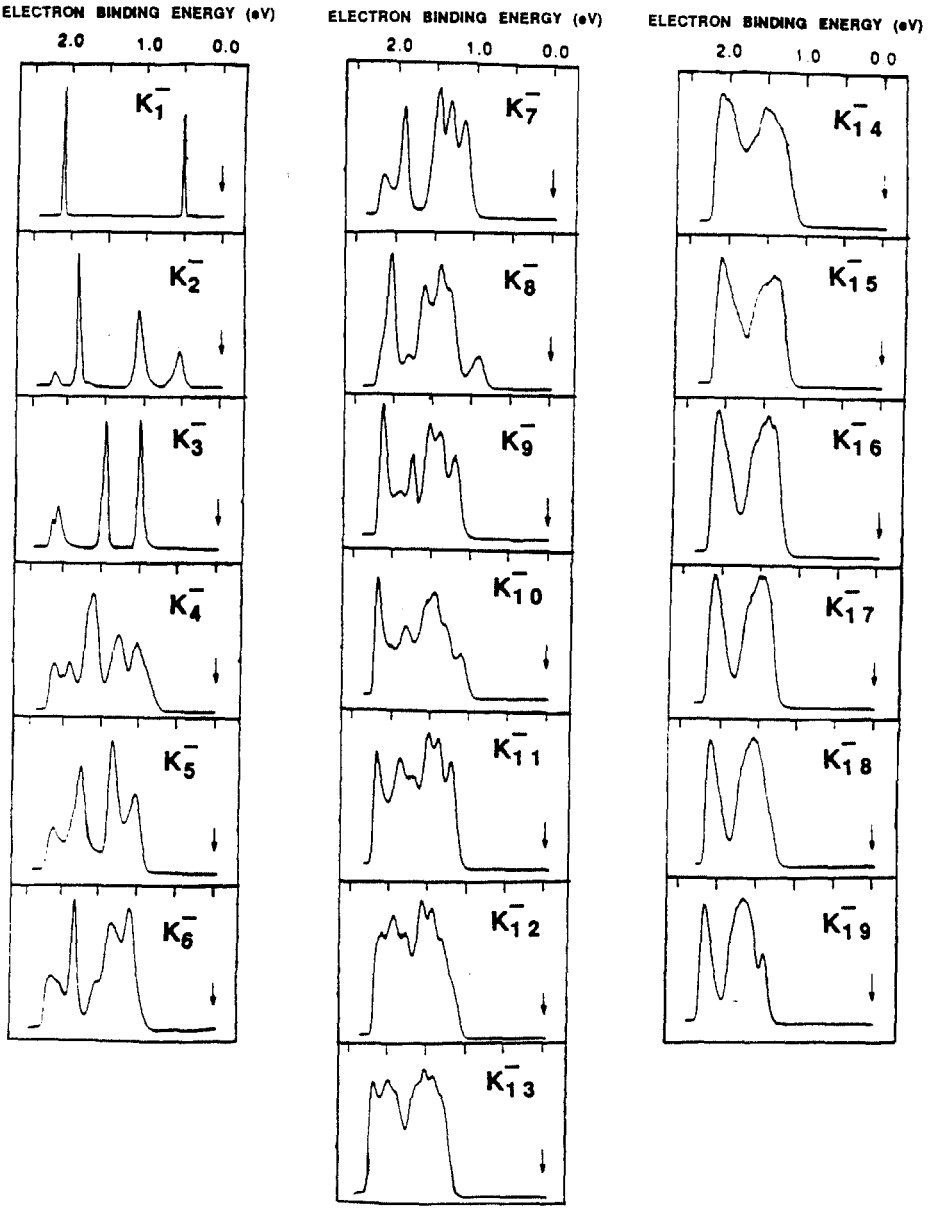

Figure 1. The photoelectron spectra of $K^-_{1\text{-}19}$ recorded with 2.540 eV photons.

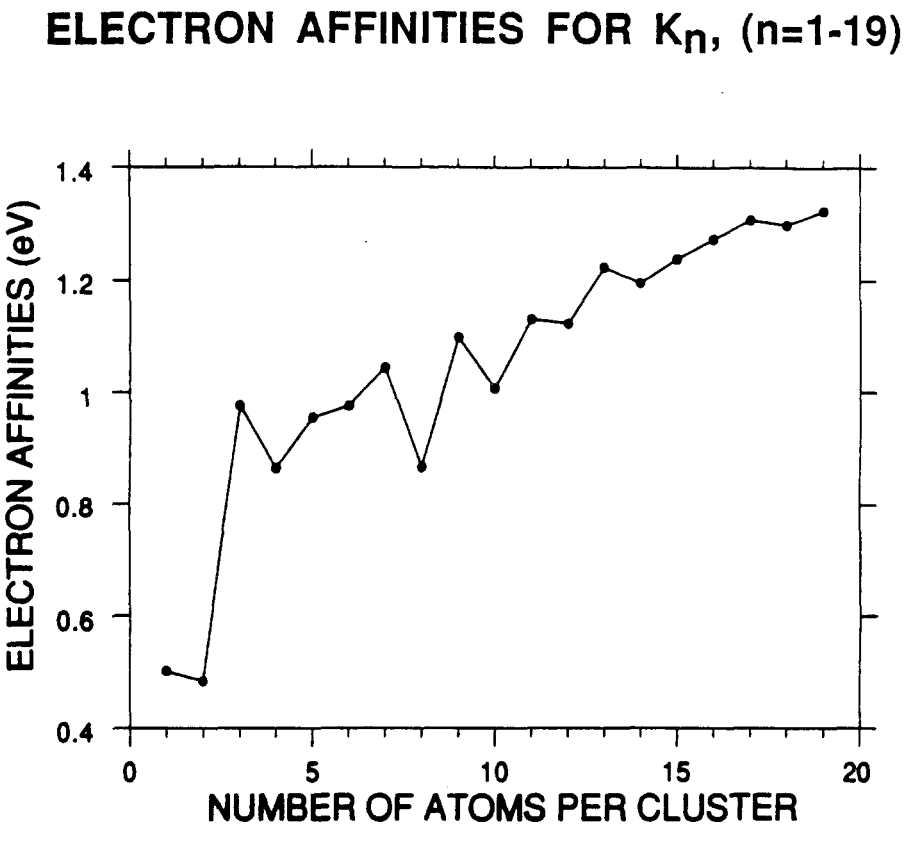

Figure 2. Measured adiabatic electron affinities of K_{1-19} as a function of cluster size.

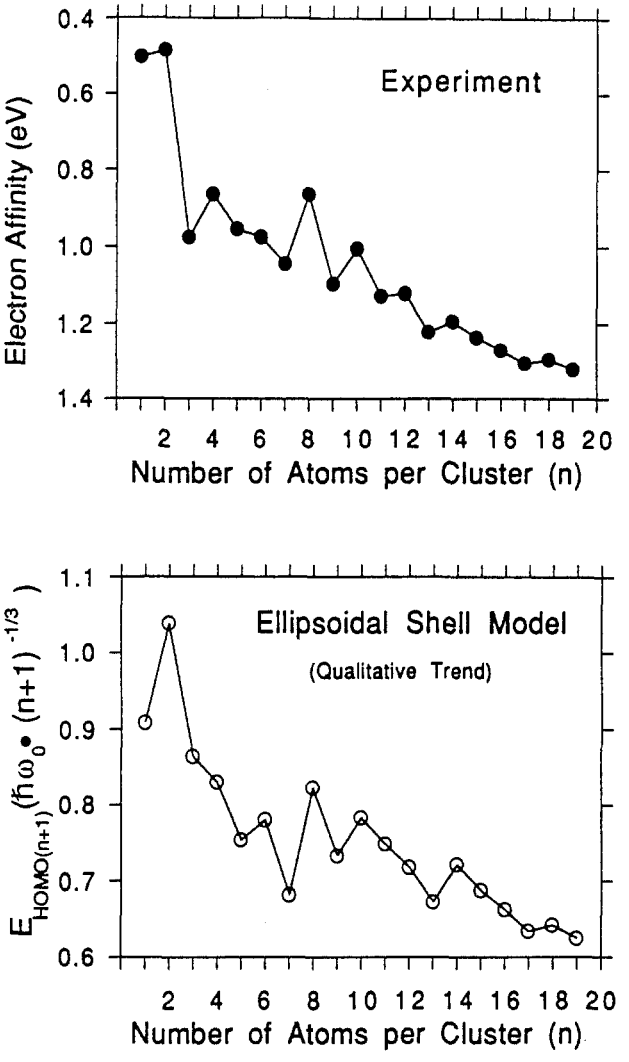

Figure 3. Comparison of the experimentally determined EA vs. n trend for $K_{n=1-19}$ (top) with the qualitative EA vs. n trend predicted by the ellipsoidal shell model (bottom). In the latter, the ellipsoidal shell model energy of the highest occupied level for the n+1 electron system is plotted as a function of cluster size, n. Note that the energy scale of the top plot has been inverted to facilitate comparison.

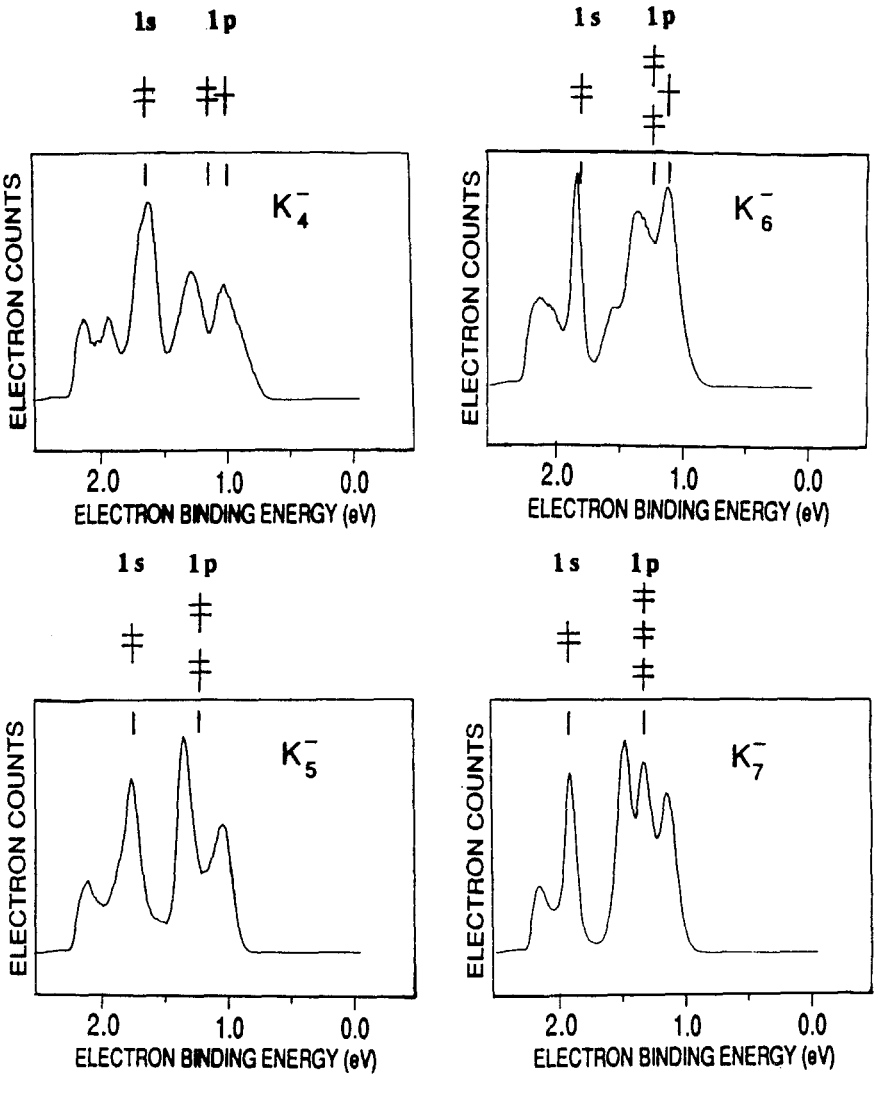

Figure 4. Comparisons of calculated shell model "stick spectra" with the corresponding observed photoelectron spectra of K_n^- (n=4-7). The "stick spectra" are shown as insets on each photoelectron spectrum. Designations and electron occupations for individual levels are shown above each "stick spectrum".

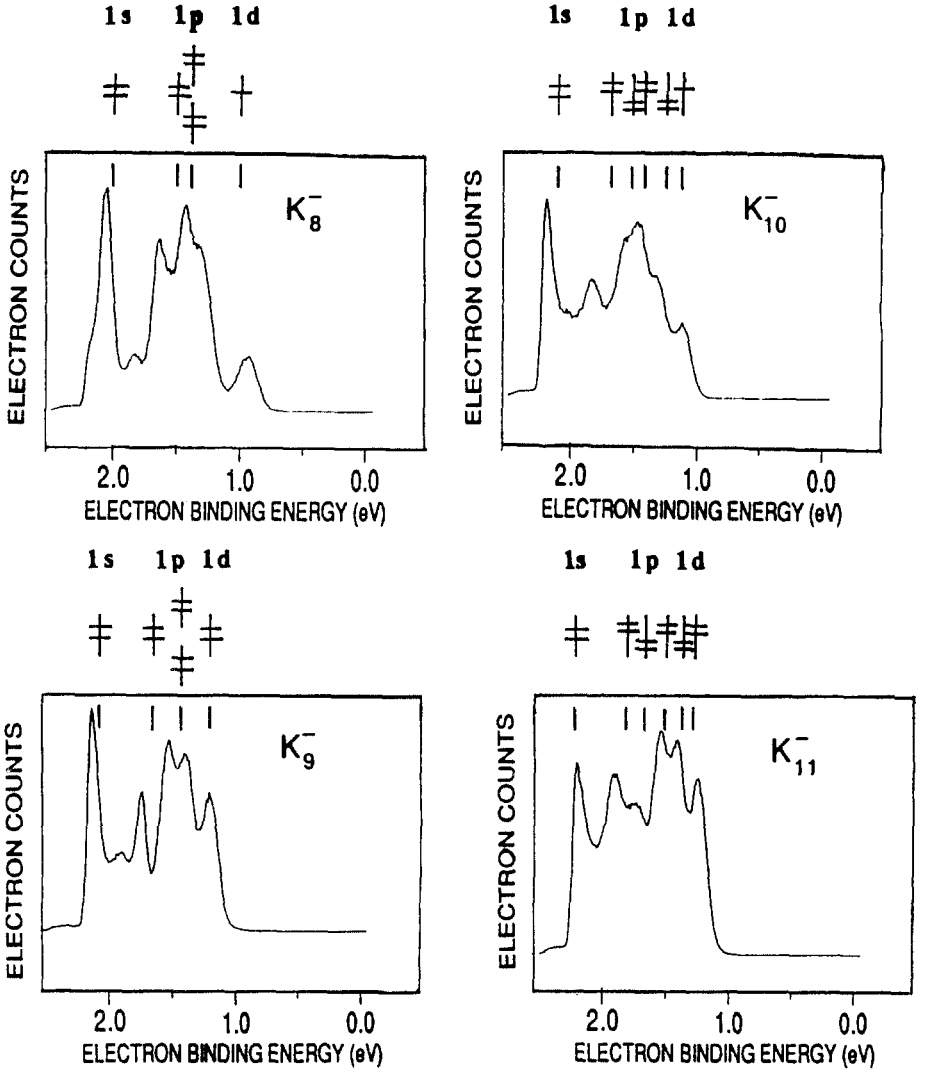

Figure 5. Comparisons of calculated shell model "stick spectra" with the corresponding observed photoelectron spectra of K_n^- (n=8-11). The "stick spectra" are shown as insets on each photoelectron spectrum. Designations and electron occupations for individual levels are shown above each "stick spectrum".

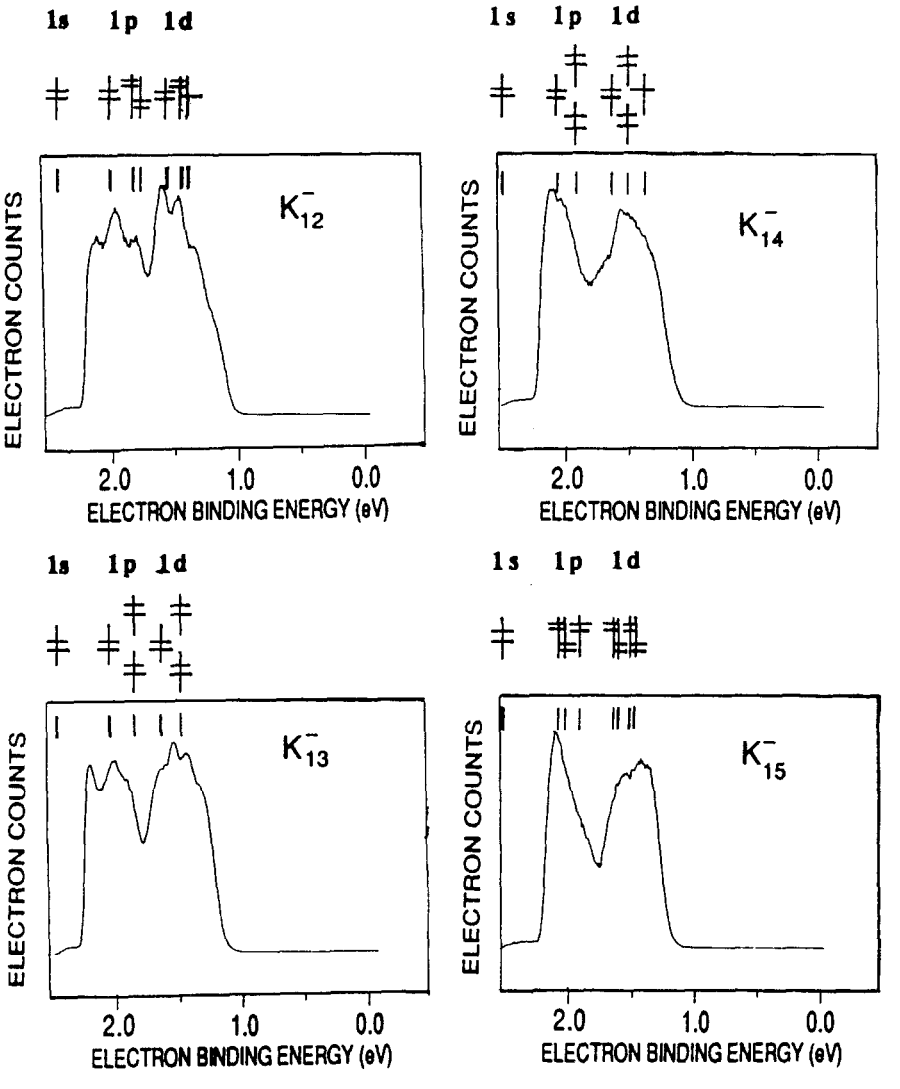

Figure 6. Comparisons of calculated shell model "stick spectra" with the corresponding observed photoelectron spectra of K_n^- (n=12-15). The "stick spectra" are shown as insets on each photoelectron spectrum. Designations and electron occupations for individual levels are shown above each "stick spectrum".

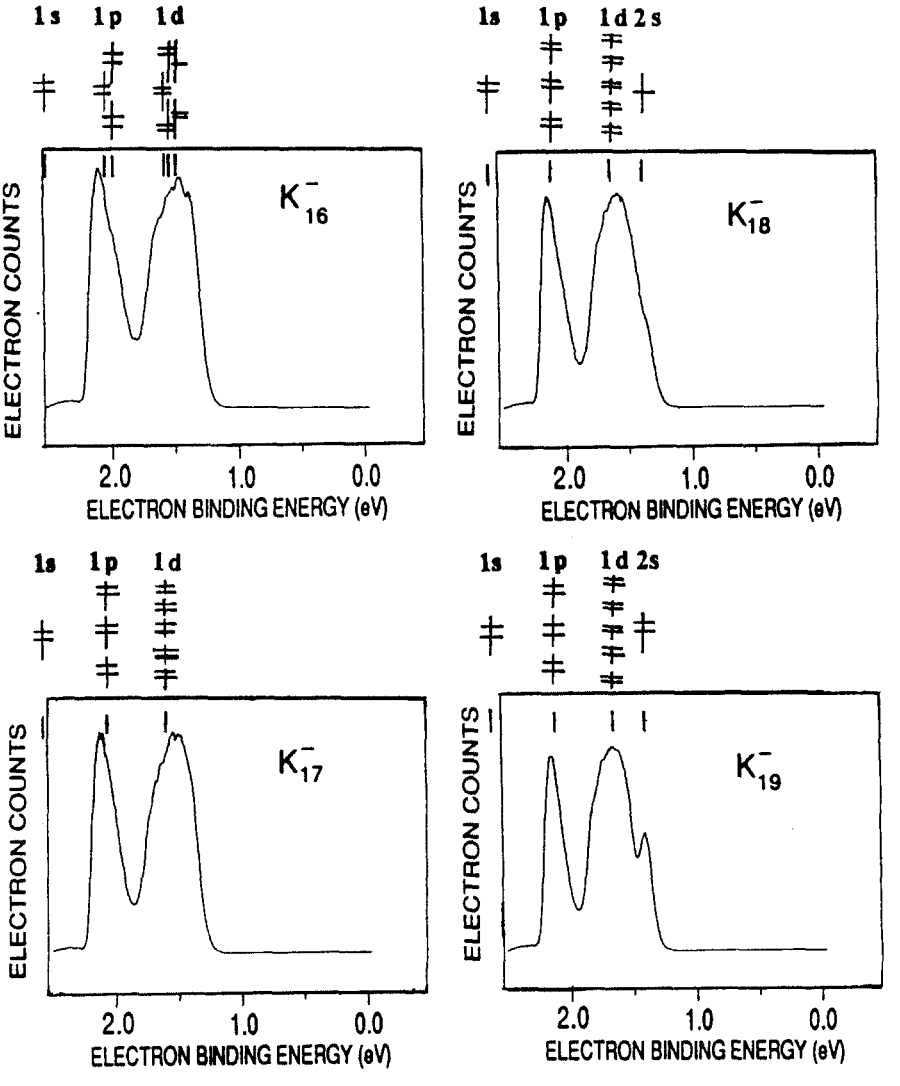

Figure 7. Comparisons of calculated shell model "stick spectra" with the corresponding observed photoelectron spectra of K_n^- (n=16-19). The "stick spectra" are shown as insets on each photoelectron spectrum. Designations and electron occupations for individual levels are shown above each "stick spectrum".